ORGANIC PROCESS RESEARCH & DEVELOPMENT
OPR&D

pubs.acs.org/OPRD

Article

Dynamic Spinning Disc Reactor Technology to Enable In Situ Solid Product Formation in a Diazotization and Azo Coupling Sequence

Dominik Polterauer, Kevin M. P. van Eeten, Wouter Stam, Christopher A. Hone,* and C. Oliver Kappe*

Cite This: *Org. Process Res. Dev.* 2024, 28, 1903−1909

Read Online

ACCESS | Metrics & More | Article Recommendations | Supporting Information

ABSTRACT: Solid-forming reactions are notoriously challenging to process in standard flow processes. Even though the formation of a solid product within a reaction can facilitate simple purification, homogeneous reactions are often utilized to enable flow processing. We report the application of dynamic spinning disc reactor (SDR) technology as a strategy to handle in situ solid product formation while handling exothermic chemistry. The system is exemplified by using a diazotization and azo coupling reaction system. Advantages of the approach include the use of water as the sole reaction solvent, mild operating conditions (20 °C), and a simple isolation procedure by filtration and drying. We demonstrate that stable operation of the system is possible for 120 min, affording 55.9 g of Sudan II.

KEYWORDS: *continuous flow, spinning disc reactor, diazotization, water, solid−liquid, azo dyes*

Diazotization reactions are important in organic synthesis, such as for the preparation of pharmaceuticals, agrochemicals, materials, and dyes.[1] Since their discovery in 1858, aryl diazonium salts have become one of the most versatile synthetic intermediates.[2] They are used in a variety of reactions, including the Sandmeyer reaction, Balz−Schiemann reaction, Pschorr cyclization, and Meerwein arylation. Despite their synthetic utility, aryl diazonium salts are highly reactive, thermally unstable, and potentially explosive.[3] Significant exotherms can be observed, and therefore, careful temperature management is necessary.[4] Consequently, they are underutilized due to the associated process challenges in handling them.

In recent years, these associated challenges have driven the development of methodologies for the handling of diazoniums in a safe and controlled manner.[5] Flow chemistry has become an established method to mitigate the risks of hazardous chemistry by handling smaller reaction volumes and providing the ability to quench a reactive intermediate in situ.[6,7] Furthermore, continuous flow reactors have larger surface to volume ratios, enabling improved heat management.[8] These reactor systems have small volumes, and therefore, less energy is needed for processing.[9] Continuous flow systems have been demonstrated to improve control over the reaction conditions (e.g., temperature and pressure).[10] Continuous flow tubular microreactors or mesoreactors are the most commonly used systems in chemical laboratories since they are widely commercially available and easy to assemble in a plug-and-play manner.[11]

The mixing within a flow reactor can be categorized as either passive or active, whereby the mixing relies on diffusion and pumping energy or provision of other external energy to achieve mixing, respectively.[12] Examples of passive mixing devices include Y- and T-pieces, tubing, multilaminating, and split-and-recombine.[13] The management of solids within continuous flow systems is a major challenge.[14] The main disadvantage of using continuous flow systems that rely on passive mixing is the usage or generation of solids during the reaction. Clogging or reactor fouling is challenging to handle in these systems when attempting to run smooth and continuous operation.[15,16] Moreover, solid accumulation can cause pressure buildup within the reactor system, which can have profound safety implications and result in process failure. Efforts to prevent blockages can lead to somewhat cumbersome cleaning and deblocking cycles or result in redevelopment of the chemistry or the avoidance of using a continuous process altogether.

The benefit of active mixing devices is that they have the ability to suspend solids and thus prevent fouling from taking place. Continuous flow stirred tank reactors (CTSRs) provide active mixing through agitators capable of suspending solids.[17−19] Oscillatory flow reactors use time-pulsing flow due to a periodic change of pumping energy, resulting in active mixing.[20,21] Agitated reactors comprise a reaction block which is mounted on a laterally shaking motor.[22] Another approach for handling solids is to use rotor−stator technology.[23] The high rotation speeds of the rotor and the small gap between the rotor and the reactor housing result in very high shear forces. A Taylor vortex flow (TVF) reactor system comprises a static cylinder shell which contains a rotating cylinder, whereby the shear is generated in the annular volume.[24,25] Stator−rotor spinning disc reactor (SDR) technology uses the very high shear forces generated by the rotation of the discs.[26] The motion within these active mixing systems counteracts the solid deposition and prevents blocking of the flow channels.

Special Issue: Flow Chemistry Enabling Efficient Synthesis 2024

Received: November 21, 2023
Revised: January 9, 2024
Accepted: February 1, 2024
Published: February 21, 2024

Since the early 2000s, several research groups have developed diazotization protocols using continuous flow reactor techniques to avoid isolating the unstable diazonium intermediates. Microreactors and mesoscale reactors based on passive mixing were used.[5,27−33] de Mello and co-workers reported the first microflow synthesis of azo dyes, but only low conversions were achieved (Scheme 1a).[28] Watts and co-worker extended this work with a comprehensive optimization study.[31] The authors used Little Things Factory (LTF) microreactors with a residence time of 2.4 min to achieve high conversion values. Subsequently, the protocol was scaled up to a mesoscale reactor (i.d. 1.5 mm), but a decrease in conversions was observed. Low concentrations and *N*,*N*-dimethylformamide (DMF) as a cosolvent were necessary to achieve a homogeneous liquid system amenable to the reactor systems. DMF should be avoided due to its potential reproductive toxicity.[34] There is regulation from the European Commission restricting the use of DMF for manufacture, which started from December 12, 2023.[35] A further limitation was that relatively limited throughput was obtained. Baxendale and co-workers made an interesting advance in handling aryl diazonium salts and solid product formation within a dynamic Coflore agitated tube reactor (ATR).[36] In that study, the researchers achieved kilogram-quantity continuous production of triacetic acid lactone solid.

Herein we outline our efforts in developing a protocol for a diazotization reaction and subsequent azo coupling using an SDR system (Scheme 1b). We selected the diazotization of 2,4-dimethylaniline (**1**) followed by an azo coupling with 2-naphthol (**2**) to form the dye Sudan II (**3**) as a model system (Scheme 2). The main focus was to achieve high conversion values while facilitating the processing of solid product formation. In addition, we were interested in using water as the sole reaction solvent due to its excellent environmental credentials.[37−39] The use of water as the only solvent could also potentially simplify purification since azo dye **3** is sparingly soluble in water. Thus, simple filtration and drying can be used to isolate the product, assuming quantitative conversion to product can be achieved.

Scheme 1. Diazotization and Azo Coupling in Flow: (a) Use of Microscale and Mesoscale Tubular Reactor Configurations (Previous Work); (b) Use of a Dynamic Spinning Disc Reactor System to Enable the Use of Water and Handling of Solid Product Formation (This Work)

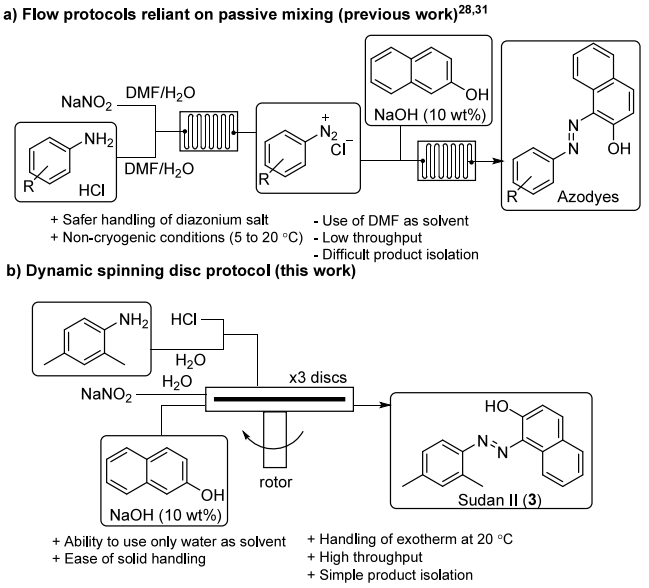

Scheme 2. Diazotization of 2,4-Dimethylaniline (1) and Subsequent Azo Coupling with 2-Naphthol (2) to Form Sudan II (3)

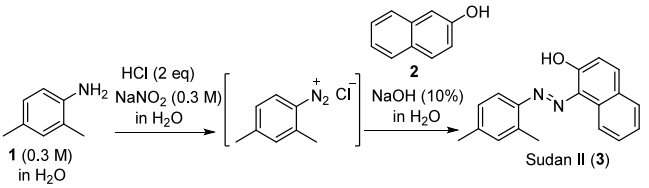

Typically, the industrial production of azo dyes is performed batchwise.[40] For direct diazotization, the aromatic amine is dissolved or suspended in aqueous acid, hydrochloric acid, or sulfuric acid. In the case of water-insoluble or partially soluble amines, then these systems can be diluted with an organic solvent. Concentrated sodium nitrite is then added. An excess of 2.5 to 3 equiv of acid is used per equivalent of amine. This protocol is performed at a temperature of 0 to 5 °C. Once the diazonium salt is formed, the coupling partner is added to the system.

We commenced our investigations with small-scale batch experiments. (***Caution:*** Diazonium salts can be unstable; therefore, care should be taken during handling.) The reactions were performed on a 0.41 mmol scale at 0 °C to prevent decomposition of the diazonium salt. 2,4-Dimethylaniline (**1**) was dissolved in water. The same equivalents of reagents (8 equiv of HCl, 4 equiv of $NaNO_2$, and 1 equiv of **2**) were used as in the study reported by Watts and co-worker.[31] We observed the immediate formation of a red solid after the addition of 2-naphthol (**2**), and >99% conversion of **2** was achieved. However, when using the equivalents (2 equiv of HCl, 1 equiv of $NaNO_2$, and 1 equiv of **2**) needed based on the reaction mechanism (Scheme S1 in the Supporting Information (SI)), only 81% conversion of **2** was observed. In both cases, a significant exotherm was observed.

The SDR technology (SpinPro R10) used in this study is commercially available from Flowid.[41] It is a type of rotor−stator spinning disc technology.[42,43] The system comprises three rotating discs (rotors) that are contained within a narrow chamber (stator). The total internal volume of the SpinProR10 is 19 mL. The material of construction of the entire rotor−stator assembly is silicon carbide, a chemically inert and corrosion-resistant material. The rotor−stator distance is 0.5 mm, while the rotor is magnetically coupled to achieve between 1001 revolutions per minute (rpm) and very high rotation speeds of up to 6000 rpm. The large velocity differential over the narrow rotor−stator gap gives rise to a high degree of turbulence, which enhances mixing on the microscopic level and[44−46] at the same time assures the continuous motion of precipitated particles to prevent blockages.

The regions near the axis of rotation (both above the disc and under the disc) can be described as radial plug flow reactors (PFRs), and the region surrounding the rim of the disc and the outer part of the reactor can be considered very well mixed, a mixed flow regime (Figure 1).[47] This technology has already been described for handling concentrated organolithium reactions. The system enabled the use of ambient

https://doi.org/10.1021/acs.oprd.3c00448
Org. Process Res. Dev. 2024, 28, 1903−1909

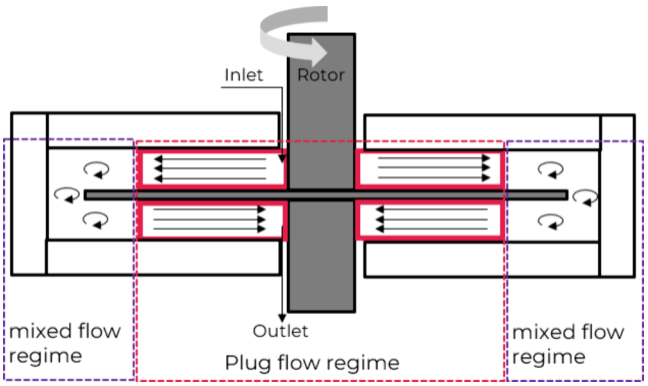

Figure 1. Simplified representation of a single-stage dynamic SDR showing the location of the flow regimes.

rather than cryogenic temperatures, and salt precipitation could be tolerated.[26]

The reactor configuration used in this study is shown in Scheme 3 (also see SI section 5). Neat **1** and 1.2 M HCl were

Scheme 3. Detailed Experimental Setup for the Diazotization and Azo Coupling in Dynamic Flow Mode[a]

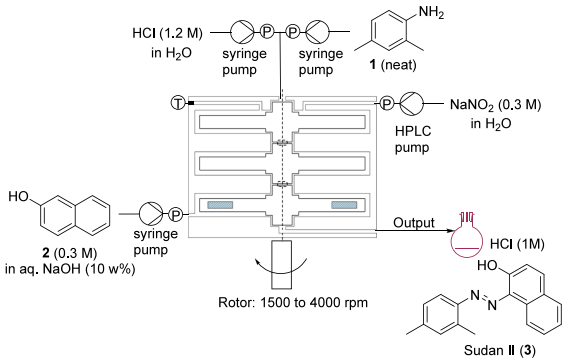

[a]T = temperature sensor. P = pressure sensor. Segment 1 (top) = 5 mL; segment 2 (middle) = 5 mL; segment 3 (bottom) = 9 mL.

mixed within a T-piece to generate a droplet flow regime prior to entering the SDR system. Syringe pumps introduced these two liquid feeds. This flow was then mixed with 0.3 M $NaNO_2$ in the first reactor segment. The first and second reactor segments were used for the diazotization reaction to form the diazonium salt intermediate. In the solid state, diazonium salts are sensitive to friction and shock; therefore, the system was configured so that the diazonium salt remained dissolved in solution and was consumed in situ. **2** was then introduced in the third reactor segment for the azo coupling, so the entire telescoped synthesis could be performed in a single reactor. The reported residence time (t_{res}) for each step was calculated based on the combined flow rates contributing to that section of the reactor (see also SI section 6.2).

The feed for **2** was a turbid solution, showing that we were at the solubility limit. We selected this concentration to maximize the productivity per unit time and per volume of reactor. The effluent then left the reactor through a short length of tubing, which was kept moving through the use of two vibration motors (see Figure S5).[48]

Initially, the same stoichiometric conditions (8 equiv of HCl, 4 equiv of $NaNO_2$, and 1 equiv of **2**) were investigated in the flow reactor as tested that provided quantitative conversion under batch conditions (Table 1, entry 1). Gratifyingly, under these conditions >99% conversion of **2** was achieved. High conversion was maintained even at half the residence time, also providing higher throughput (entry 2). We were interested in observing whether we could decrease the equivalents of the reagents to make the reaction more efficient. A reduction in equivalents did provide quantitative conversion (entries 3−5). We validated that high conversion values for **2** corresponded to achieving a high yield of **3** by performing an isolation for an experiment (entry 3). The collected fractions were combined, filtered, and then dried to provide 99% isolated yield. On using the theoretical needed equivalents (2 equiv of HCl, 1 equiv of $NaNO_2$, and 1 equiv of **1**) based on the reaction mechanism, a drop in conversion to 86% was observed (entry 6), which was slightly higher than observed under batch conditions. The equivalents of reagents which were found to be sufficient to provide 99% conversion of **2** were 2.4 equiv of HCl, 1.2 equiv of $NaNO_2$, and 1.2 equiv of **1** (entry 7), and these were used for further optimization.

Subsequently, experiments were performed to identify the best temperature, rotation speed, and residence time (Table 2). Residual starting material was observed when operating at a low temperature (2 °C) (entry 1). An additional batch experiment performed with the same equivalents of the reagents resulted in a 92% conversion of **2**. Quantitative conversion was obtained both at 20 and 40 °C in the SDR system (entries 2 and 3). Gratifyingly, on operation at half the residence time, thus doubling the throughput, quantitative conversion was maintained (entry 4). The combined residence time for the two steps could be decreased to 1.3 min without compromising the conversion (entry 5). However, lowering the combined residence time to 0.9 min resulted in a marginal drop in conversion (entry 7). On increasing the rotation speed to 4000 rpm, a very slight decrease in the conversion of **2** was observed (cf. entries 5 and 6 and entries 7 and 8). Although the effect is relatively small, it is in line with theory. When increasing the disc speed, turbulence intensity and micromixing are increased, leading to a growth of the volume of the well-mixed region at the expense of the volume of the plug flow regime. The well-mixed region has more back-mixing than the PFR region, resulting in a small decrease in reaction rate.[47] We selected the following conditions to validate the system in a robustness experiment: a temperature of 20 °C, a rotation speed of 3000 rpm, and a combined residence time of 1.5 min for the two steps (entry 4). This corresponded to flow rate values of 0.262 mL/min for aniline **1**, 3.40 mL/min for aqueous HCl, 6.86 mL/min for aqueous sodium nitrite, and 5.69 mL/min for **2**.

We assessed the flow regime that would be observed under the conditions explored in this study. Two dimensionless numbers are required to determine the flow regime, the Reynolds number (Re) and the rotor−stator gap ratio (G):

$$Re = \omega R_D^{\,2} \nu^{-1} \quad (1)$$

$$G = \frac{h}{R_D} \quad (2)$$

where ω is the disc speed (rad/s, whereby 3000 rpm = 314 rad/s), R_D is the radius of the rotor (35 mm), ν is the kinematic viscosity in water (1 mm^2/s), and h is the rotor−stator gap (0.5 mm). Daily and Nece performed detailed experimental studies and observed that four regimes are possible in rotor−stator cavities (Figure 2).[49] A Reynolds

https://doi.org/10.1021/acs.oprd.3c00448
Org. Process Res. Dev. 2024, 28, 1903−1909

Table 1. Stoichiometry Optimization for the Diazotization and Azo Coupling[a]

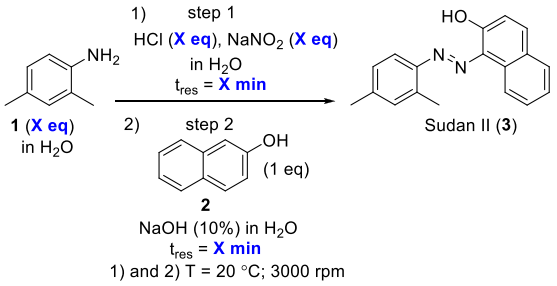

entry	equiv of HCl	equiv of $NaNO_2$	equiv of **1**	t_{res} [min] step 1	t_{res} [min] step 2	conv. of **2** [%][b]	throughput [g/h][c]
1	8	4	2	2.5	1.9	>99	3.4
2	8	4	2	1.2	0.9	>99	6.8
3	5.8	3	1.5	1.9	1.4	>99(99)	5.7
4	3.9	2	1.2	1.7	1.2	>99	9.5
5	2.7	1.4	1.4	1.9	1.2	>99	12.5
6	2	1	1	3.4	1.9	86	9.5
7	2.4	1.2	1.2	1.9	1.1	>99	14.3

[a]Fixed conditions are shown in the scheme. See Table S4 for pump flow rates. [b]Conversion of **2** was assessed by HPLC-UV. The number in parentheses corresponds to the isolated yield of **3**. [c]Theoretical product throughput based on 100% yield.

Table 2. Flow Optimization for the Diazotization and Azo Coupling[a]

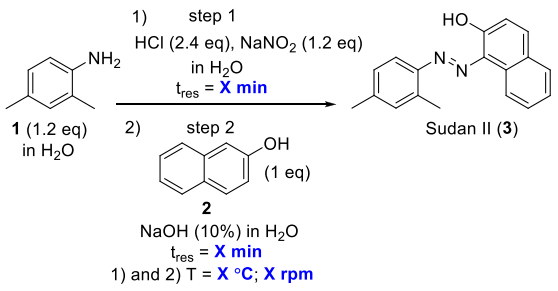

entry	T [°C]	rotation speed [rpm]	t_{res} [min] step 1	t_{res} [min] step 2	conv. of **2** [%][b]	throughput [g/h][c]
1	2	3000	1.9	1.1	99	14.3
2	20	3000	1.9	1.1	>99	14.3
3	40	3000	1.9	1.1	>99	14.3
4	20	3000	0.9	0.6	>99 (98)	28.5
5	20	3000	0.7	0.4	>99	38.0
6	20	4000	0.7	0.4	98	38.0
7	20	3000	0.6	0.3	98	47.5
8	20	4000	0.6	0.3	97	47.5

[a]Fixed conditions are shown in the scheme. See Table S4 for pump flow rates. [b]Conversion of **2** was assessed by HPLC-UV. The number in parentheses corresponds to the isolated yield of **3** from the final long run. [c]Theoretical product throughput based on 100% yield.

number of 3.85×10^5 and a gap ratio of 0.0143 were calculated, which locates our flow regime in the middle of Regime III (see the dot in Figure 2). This regime is the best for dynamic SDR technology because it has a high degree of turbulence and a nearly uniform distribution of shear. The two left flow regimes (I and II) on the map are laminar, and the upper right regime (IV) has the shear rates concentrated in the boundary layers near the rotor and stator (i.e., the shear is not well-distributed). Even at a disc speed of 1000 rpm (Re = 1.28×10^5; G remained unchanged) or 6000 rpm (Re = $7.70 \times$

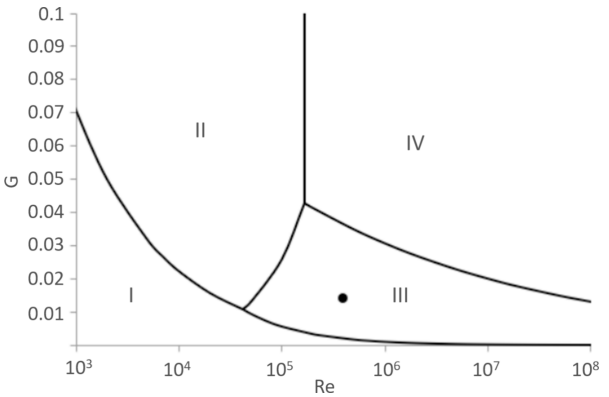

Figure 2. Flow regimes in the rotor−stator cavities according to Daily and Nece[49] and Launder et al.[50] The dot shown in regime III was calculated using the values shown in the text. Roman numerals refer to the flow regimes: Regime I, laminar flow with merged boundaries; Regime II, laminar flow with separated boundaries; Regime III, turbulent flow with merged boundaries; Regime IV, turbulent flow with separated boundaries.

10^5), we stay well within Regime III. Thus, for this reaction, which occurs as a single liquid-phase process until the precipitation of azo dye **3**, the disc speed is not expected to have a large influence on the yield and selectivity. These calculations are in agreement with the experimental tests we performed at lower and higher disc speeds.

The thermal behavior of the diazotization and azo coupling steps were both measured using a micro reaction batch calorimeter (see SI section S3). The experiment revealed a heat of reaction (ΔH_{rxn}) of −127 kJ mol^{-1} for the first step, thus demonstrating its exothermic nature, which corresponds to an adiabatic temperature rise of 18.5 °C. This result highlights the importance of controlling the exotherm through careful dosing of reagents and good heat transfer given the thermal instability of diazonium salts, which then can result in the evolution of nitrogen gas on decomposition.[3,4,51] For the second step, an exotherm was also observed, which is a

https://doi.org/10.1021/acs.oprd.3c00448
Org. Process Res. Dev. 2024, 28, 1903−1909

combination of the exothermic neutralization of HCl and NaOH (between −56 and −58 kJ/mol based on literature references)[52−54] and the endothermic azo coupling (35.6 kJ/mol).

Subsequently, we were interested in demonstrating the robustness of our optimized conditions over a longer operation time in a scale-out experiment. Efforts were initially made with the same setup used during the optimization campaign. This setup included the use of a 1/8 in. connector and tubing at the outlet. The initial attempts to operate the system for a prolonged operation time resulted in a gradual pressure buildup caused by the accumulation of solid within the system. This buildup led us to stop the experiment after 37 min. To gain further insight into the solid buildup, we evaluated the particle size distribution over the run time of the solids within the collected fractions using laser diffraction of the solids within. For fractions 1 to 2, a volume mean diameter (VMD) of ∼16 μm was measured, whereas later in the operation, particularly for fraction 4, the collected product was observed to have two distinct VMD values of ∼22 and ∼100 μm (Figure 3). The larger of these particles led to complications in handling over more extended periods due to settling in the outlet tube inside the reactor. To address this issue, we aimed to reduce the mean particle size by preventing agglomeration and pressure buildup, thus enabling more stable processing.

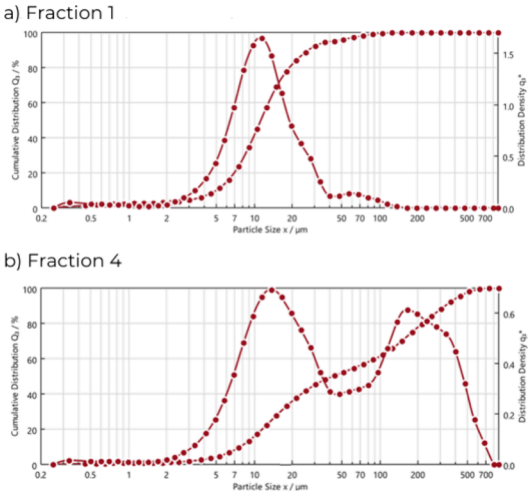

Figure 3. Particle size distribution laser diffraction results for fractions 1 and 4 from the first attempted long run. Fractions were collected at 10 min intervals.

To avoid blockages, we further modified our setup by introducing check valves at all the pumps and by using a 1/4 in. connector and tubing at the outlet. The monitoring of the pressure readings during operation showed a variable pressure profile. A couple of times during the run, the pressure increased to 2.5 bar, presumably due to partial channel blockages. Gratifyingly, this pressure was released after a certain amount of time, returning the system to its normal level. Pump pulsation can result in a change in the reagent stoichiometry. In contrast to the earlier results, measuring the particle size distribution revealed a single distinct VMD value of ∼38 ± 6 μm (average based on measurements for 12 fractions) over the entire experiment (see SI section 6.4.2). The long run demonstrated that the protocol was stable for 120 min and afforded 55.9 g of **3** (98% isolated yield) after filtration and drying. This value corresponds to a throughput of 28.5 g/h and a potential throughput of 684 g/day. Considering the 19 mL of total reactor volume, a space-time yield of 1.5 kg L^{-1} h^{-1} was achieved.

Our main goal was to demonstrate the viability of performing this type of chemistry within an SDR system. We believe that the pulsation from the syringe pumps could be partially responsible for the changes in pressure, as the dosing of reagents fluctuated, leading to small changes in reagent stoichiometry. However, these changes in pressure did not compromise the conversion of **2**. Implementing mass flow meters would enable more careful monitoring of the reagent stoichiometry.[55] These data could then be used to help gain information regarding the pump performance and pressure buildup. The use of gear pumps or HPLC pumps would also reduce the pulsation effects. Moreover, when scaling up the application to full industrial size, the diameter of the piping and connectors will need to increase as well, further limiting the possibility of particle accumulation. For a continuous manufacturing application, this would thus give confidence that this solid-forming process can run uninterruptedly in flow during the entire length of a production campaign. The resulting space-time yield of 1.5 kg L^{-1} h^{-1} in the lab-scale SpinPro R10 can be readily translated linearly to a scaled-up industrial process because of the hydrodynamic and geometric self-similarity that underlies the engineering and design principles of the entire SpinPro platform. Moreover, qualitatively similar yields and selectivities are obtained when the following parameters are kept constant when scaling up: Reynolds number, shear rate ratio between the rotor−stator gap and the disc radius, and heat transfer.[45−47] Mixing behavior can be predicted and compared using a flow regime map to ensure similar results at different scales. In a SpinPro R300, for example, this will lead to a production rate of **3** of 8.28 kg/day using a reactor volume of 230 mL.

In summary, we describe the development of a diazotization and azo coupling within a dynamic spinning disc system. The reactor system enables the process to be performed in a safer and more controlled manner compared to batch systems. In addition, this approach enables the use of water as the sole solvent for preparing azo dyes. In particular, the system facilitated the handling of in situ solid product within the reactor system due to the high shear forces present. The product was isolated by simple filtration and drying. The system was successfully demonstrated in a long run. In a very recent review by Stephens and co-worker, they highlighted successful step-up of a continuous flow process for azo generation has not been reported.[56]

We believe that the results discussed in our report represent a significant advance in improving the processibility and scalability of azo generation.We hope that these results will increase the confidence in performing multiphase reactions, especially those involving solids (e.g., suspensions and slurries), in (continuous) chemical manufacturing environments.

■ ASSOCIATED CONTENT

Data Availability Statement

The data underlying this study are available in the published article and its online Supporting Information.

Supporting Information

The Supporting Information is available free of charge at https://pubs.acs.org/doi/10.1021/acs.oprd.3c00448.

https://doi.org/10.1021/acs.oprd.3c00448
Org. Process Res. Dev. 2024, 28, 1903−1909

Detailed description of the flow configuration, synthetic procedures, reaction optimization data, compound characterization data, and copies of NMR spectra (PDF)

AUTHOR INFORMATION

Corresponding Authors

Christopher A. Hone − *Center for Continuous Flow Synthesis and Processing, Research Center Pharmaceutical Engineering GmbH, A-8010 Graz, Austria; Institute of Chemistry, NAWI Graz, University of Graz, A-8010 Graz, Austria;* orcid.org/0000-0002-5939-920X; Email: christopher.hone@rcpe.at

C. Oliver Kappe − *Center for Continuous Flow Synthesis and Processing, Research Center Pharmaceutical Engineering GmbH, A-8010 Graz, Austria; Institute of Chemistry, NAWI Graz, University of Graz, A-8010 Graz, Austria;* orcid.org/0000-0003-2983-6007; Email: oliver.kappe@uni-graz.at

Authors

Dominik Polterauer − *Center for Continuous Flow Synthesis and Processing, Research Center Pharmaceutical Engineering GmbH, A-8010 Graz, Austria; Institute of Chemistry, NAWI Graz, University of Graz, A-8010 Graz, Austria;* orcid.org/0000-0003-0131-8224

Kevin M. P. van Eeten − *Flowid B.V., 5301 LW Zaltbommel, The Netherlands*

Wouter Stam − *Flowid B.V., 5301 LW Zaltbommel, The Netherlands*

Complete contact information is available at: https://pubs.acs.org/10.1021/acs.oprd.3c00448

Author Contributions

The manuscript was written through contributions of all authors. All of the authors approved the final version of the manuscript.

Notes

The authors declare no competing financial interest.

ACKNOWLEDGMENTS

The Research Center Pharmaceutical Engineering is funded within the framework of COMET Competence Centers for Excellent Technologies by BMK, BMDW, Land Steiermark, and SFG. The COMET Program is managed by the FFG. Dr. Doris Dallinger is gratefully acknowledged for her advice during the project.

REFERENCES

(1) Mo, F.; Qiu, D.; Zhang, L.; Wang, J. Recent Development of Aryl Diazonium Chemistry for the Derivatization of Aromatic Compounds. *Chem. Rev.* **2021**, *121*, 5741−5829.

(2) Griefs, P. Vorläufige Notiz über die Einwirkung von salpetriger Säure auf Amidinitro- und Aminitrophenylsäure. *Justus Liebigs Ann. Chem.* **1858**, *106*, 123−125.

(3) Sheng, M.; Frurip, D.; Gorman, D. Reactive chemical hazards of diazonium salts. *J. Loss Prev. Process Ind.* **2015**, *38*, 114−118.

(4) Xie, C.; Yuan, Y.; Wang, B.; Du, L. Research on the decomposition kinetics and thermal hazards of aniline diazonium salt. *Thermochim. Acta* **2022**, *709*, 179156.

(5) Chen, J.; Xie, X.; Liu, J.; Yu, Z.; Su, W. Revisiting aromatic diazotization and aryl diazonium salts in continuous flow: highlighted research during 2001−2021. *React. Chem. Eng.* **2022**, *7*, 1247−1275.

(6) Movsisyan, M.; Delbeke, E. I. P.; Berton, J. K. E. T.; Battilocchio, C.; Ley, S. V.; Stevens, C. V. Taming hazardous chemistry by continuous flow technology. *Chem. Soc. Rev.* **2016**, *45*, 4892−4928.

(7) Kockmann, N.; Thenée, P.; Fleischer-Trebes, C.; Laudadio, G.; Noël, T. Safety Assessment in Development and Operation of Modular Continuous-Flow Processes. *React. Chem. Eng.* **2017**, *2*, 258−280.

(8) Capaldo, L.; Wen, Z.; Noël, T. A field guide to flow chemistry for synthetic organic chemists. *Chem. Sci.* **2023**, *14*, 4230−4247.

(9) Bennett, J. A.; Campbell, Z. S.; Abolhasani, M. Role of continuous flow processes in green manufacturing of pharmaceuticals and specialty chemicals. *Curr. Opin. Chem. Eng.* **2019**, *26*, 9−19.

(10) Plutschack, M. B.; Pieber, B.; Gilmore, K.; Seeberger, P. H. *Chem. Rev.* **2017**, *117*, 11796−11893.

(11) Hone, C. A.; Kappe, C. O. Towards the Standardization of Flow Chemistry Protocols for Organic Reactions. *Chem. - Methods* **2021**, *1*, 454−467.

(12) Hessel, V.; Löwe, H.; Schönfeld, F. Micromixers—a review on passive and active mixing principles *Chem. Eng. Sci.* **2005**, *60*, 2479−2501.

(13) Schwolow, S.; Hollmann, J.; Schenkel, B.; Röder, T. Application-Oriented Analysis of Mixing Performance in Microreactors. *Org. Process Res. Dev.* **2012**, *16*, 1513−1522.

(14) Hartman, R. L. Managing Solids in Microreactors for the Upstream Continuous Processing of Fine Chemicals. *Org. Process Res. Dev.* **2012**, *16*, 870−887.

(15) Schoenitz, M.; Grundemann, L.; Augustin, W.; Scholl, S. Fouling in microstructured devices: a review. *Chem. Commun.* **2015**, *51*, 8213−8228.

(16) Besenhard, M. O.; Pal, S.; Gkogkos, G.; Gavriilidis, A. Non-fouling flow reactors for nanomaterial synthesis. *React. Chem. Eng.* **2023**, *8*, 955−977.

(17) Mo, Y.; Jensen, K. F. A miniature CSTR cascade for continuous flow of reactions containing solids. *React. Chem. Eng.* **2016**, *1*, 501−507.

(18) Chapman, M. R.; Kwan, M. H. T.; King, G.; Jolley, K. E.; Hussain, M.; Hussain, S.; Salama, I. E.; González Niño, C.; Thompson, L. A.; Bayana, M. E.; Clayton, A. D.; Nguyen, B. N.; Turner, N. J.; Kapur, N.; Blacker, A. J. Simple and Versatile Laboratory Scale CSTR for Multiphasic Continuous-Flow Chemistry and Long Residence Times. *Org. Process. Res. Dev.* **2017**, *21*, 1294−1301.

(19) Cherkasov, N.; Adams, S. J.; Bainbridge, E. G. A.; Thornton, J.A. M. Continuous stirred tank reactors in fine chemical synthesis for efficient mixing, solids-handling, and rapid scale-up. *React. Chem. Eng.* **2023**, *8*, 266−277.

(20) Bianchi, P.; Williams, J. D.; Kappe, C. O. Oscillatory flow reactors for synthetic chemistry applications. *J. Flow Chem.* **2020**, *10*, 475−490.

(21) Mazubert, A.; Aubin, J.; Elgue, S.; Poux, M. Intensification of waste cooking oil transformation by transesterification and esterification reactions in oscillatory baffled and microstructured reactors for biodiesel production. *Green Process Synth.* **2014**, *3*, 419−429.

(22) Browne, D. L.; Deadman, B. J.; Ashe, R.; Baxendale, I. R.; Ley, S. V. Continuous Flow Processing of Slurries: Evaluation of an Agitated Cell Reactor. *Org. Process Res. Dev.* **2011**, *15*, 693−697.

(23) Atiemo-Obeng, V. A.; Calabrese, R. V. Rotor-Stator Mixing Devices. In *Handbook of Industrial Mixing: Science and Practice*; John Wiley & Sons, 2004; Chapter 8, pp 345−390. DOI: 10.1002/0471451452.ch8.

(24) Schrimpf, M.; Esteban, J.; Warmeling, H.; Färber, T.; Behr, A.; Vorholt, A. J. Taylor-Couette reactor: Principles, design, and applications. *AIChE J.* **2021**, *67*, No. e17228.

(25) Hosoya, M.; Tanaka, M.; Manaka, A.; Nishijima, S.; Tsuno, N. Integration of Liquid−Liquid Biphasic Flow Alkylation and Continuous Crystallization Using Taylor Vortex Flow Reactors. *Org. Process Res. Dev.* **2022**, *26*, 1531−1544.

(26) Wietelmann, U.; Klösener, J.; Rittmeyer, P.; Schnippering, S.; Bats, H.; Stam, W. Continuous Processing of Concentrated Organolithiums in Flow Using Static and Dynamic Spinning Disc Reactor Technologies. *Org. Process Res. Dev.* **2022**, *26*, 1422−1431.
(27) Oger, N.; Le Grognec, E.; Felpin, F.-X. Handling diazonium salts in flow for organic and material chemistry. *Org. Chem. Front.* **2015**, *2*, 590−614.
(28) Wootton, R. C. R.; Fortt, R.; de Mello, A. J. On-chip generation and reaction of unstable intermediates—monolithic nanoreactors for diazonium chemistry: Azodyes. *Lab Chip* **2002**, *2*, 5−7.
(29) Fortt, R.; Wootton, R. C. R.; de Mello, A. J. Continuous-Flow Generation of Anhydrous Diazonium Species: Monolithic Microfluidic Reactors for the Chemistry of Unstable Intermediates. *Org. Process Res. Dev.* **2003**, *7*, 762−768.
(30) Hu, T.; Baxendale, I. R.; Baumann, M. Exploring Flow Procedures for Diazonium Formation. *Molecules* **2016**, *21*, 918.
(31) Akwi, F. M.; Watts, P. The in situ generation and reactive quench of diazonium compounds in the synthesis of azo compounds in microreactors. *Beilstein J. Org. Chem.* **2016**, *12*, 1987−2004.
(32) Liu, Y.; Zeng, C.; Wang, C.; Zhang, L. Continuous diazotization of aromatic amines with high acid and sodium nitrite concentrations in microreactors. *J. Flow Chem.* **2018**, *8*, 139−146.
(33) Wang, F.-J.; Huang, J.-P.; Xu, J.-H. Continuous-Flow Synthesis of the Azo Pigment Yellow 14 Using a Three-Stream Micromixing Process. *Org. Process Res. Dev.* **2019**, *23*, 2637−2646.
(34) Bryan, M. C.; Dunn, P. J.; Entwistle, D.; Gallou, F.; Koenig, S. G.; Hayler, J. D.; Hickey, M. R.; Hughes, S.; Kopach, M. E.; Moine, G.; Richardson, P.; Roschangar, F.; Steven, A.; Weiberth, F. J. Key Green Chemistry research areas from a pharmaceutical manufacturers' perspective revisited. *Green Chem.* **2018**, *20*, 5082−5103.
(35) *European Commission: new restriction for DMF (N,N-dimethylformamide) published on the official Gazette*. TEAM mastery S.r.l., December 21, 2021. https://www.team-mastery.eu/european-commission-new-restriction-for-dmf-nn-dimethylformamide-published-on-the-official-gazzette/ (accessed 2023-12-19).
(36) Filipponi, P.; Gioiello, A.; Baxendale, I. R. Controlled Flow Precipitation as a Valuable Tool for Synthesis. *Org. Process Res. Dev.* **2016**, *20*, 371−375.
(37) Henderson, R. K.; Jiménez-González, C.; Constable, D. J.; Alston, S. R.; Inglis, G. G. A.; Fisher, G.; Sherwood, J.; Binks, S. P.; Curzons, A. D. Expanding GSK's solvent selection guide − embedding sustainability into solvent selection starting at medicinal chemistry. *Green Chem.* **2011**, *13*, 854−862.
(38) Prat, D.; Pardigon, O.; Flemming, H.-W.; Letestu, S.; Ducandas, V.; Isnard, P.; Guntrum, E.; Senac, T.; Ruisseau, S.; Cruciani, P.; Hosek, P. Sanofi's Solvent Selection Guide: A Step Toward More Sustainable Processes. *Org. Process Res. Dev.* **2013**, *17*, 1517−1525.
(39) Simon, M.-O.; Li, C.-J. Green chemistry oriented organic synthesis in water. *Chem. Soc. Rev.* **2012**, *41*, 1415−1427.
(40) Hunger, K.; Mischke, P.; Rieper, W.; Zhang, S. Azo Dyes, 1. General. In *Ullmann's Encyclopedia of Industrial Chemistry*; Wiley, 2017. DOI: 10.1002/14356007.a03_245.pub3.
(41) *SpinPro Reactor*. https://www.flowid.nl/spinpro/ (accessed 2023-10-18).
(42) Manzano Martínez, A. N.; van Eeten, K. M.P.; Schouten, J. C.; van der Schaaf, J. Micromixing in a Rotor−Stator Spinning Disc Reactor. *Ind. Eng. Chem. Res.* **2017**, *56*, 13454−13460.
(43) Haseidl, F.; Pottbäcker, J.; Hinrichsen, O. Gas−Liquid mass transfer in a rotor−stator spinning disc reactor: Experimental study and correlation. *Chem. Eng. Process* **2016**, *104*, 181−189.
(44) Manzano Martínez, A. N.; van Eeten, K. M. P.; Schouten, J. C.; van der Schaaf, J. Micromixing in a Rotor−Stator Spinning Disc Reactor. *Ind. Eng. Chem. Res.* **2017**, *56*, 13454−13460.
(45) Manzano Martínez, A. N.; van Eeten, K. M. P.; Schouten, J. C.; van der Schaaf, J. Additions to "Micromixing in a Rotor-Stator Spinning Disc Reactor. *Ind. Eng. Chem. Res.* **2020**, *59*, 16095−16097.
(46) Hop, C. J. W.; Jansen, R.; Besten, M.; Chaudhuri, A.; Baltussen, M. W.; van der Schaaf, J. Hydrodynamics of a rotor−stator spinning disk reactor: Investigations by large-eddy simulation. *Phys. Fluids* **2023**, *35*, No. 035105.
(47) de Beer, M. M.; Keurentjes, J. T. F.; Schouten, J. C.; van der Schaaf, J. Engineering model for single-phase flow in a multi-stage rotor−stator spinning disc reactor. *Chem. Eng. J.* **2014**, *242*, 53−61.
(48) Pomberger, A.; Mo, Y.; Nandiwale, K. Y.; Schultz, V. L.; Duvadie, R.; Robinson, R. I.; Altinoglu, E. I.; Jensen, K. F. A Continuous Stirred-Tank Reactor (CSTR) Cascade for Handling Solid-Containing Photochemical Reactions. *Org. Process Res. Dev.* **2019**, *23*, 2699−2706.
(49) Daily, J. W.; Nece, R. E. Chamber dimension effects on induced flow and frictional resistance of enclosed rotating disks. *ASME J. Fluids Eng.* **1960**, *82*, 217−230.
(50) Launder, B.; Poncet, S.; Serre, E. Laminar, transitional, and turbulent flows in rotor−stator cavities. *Annu. Rev. Fluid Mech.* **2010**, *42*, 229−248.
(51) Schotten, C.; Leprevost, S. K.; Yong, L. M.; Hughes, C. E.; Harris, K. D. M.; Browne, D. L. Comparison of the Thermal Stabilities of Diazonium Salts and Their Corresponding Triazenes. *Org. Process Res. Dev.* **2020**, *24*, 2336−2341.
(52) Frede, T. A.; Dietz, M.; Kockmann, N. Software-Guided Microscale Flow Calorimeter for Efficient Acquisition of Thermokinetic Data. *J. Flow Chem.* **2021**, *11*, 321−332.
(53) Romano, M.; Pradere, C.; Sarrazin, F.; Toutain, J.; Batsale, J. C. Enthalpy, Kinetics and Mixing Characterization in Droplet-Flow Millifluidic Device by Infrared Thermography. *Chem. Eng. J.* **2015**, *273*, 325−332.
(54) Frede, T. A.; vom Hofe, N.; Reuß, R. J.; Kemmerling, N.; Kock, T.; Herbstritt, F.; Kockmann, N. Design and Characterization of a Flow Reaction Calorimeter Based on FlowPlate® Lab and Peltier Elements. *React. Chem. Eng.* **2023**, *8*, 1051−1060.
(55) Sagmeister, P.; Williams, J. D.; Hone, C. A.; Kappe, C. O. Laboratory of the future: a modular flow platform with multiple integrated PAT tools for multistep reactions. *React. Chem. Eng.* **2019**, *4*, 1571−1578.
(56) McCormack, A. T.; Stephens, J. C. The continuous flow synthesis of azos. *J. Flow Chem.* **2024**, DOI: 10.1007/s41981-024-00307-2.

NOTE ADDED AFTER ASAP PUBLICATION

This paper was published ASAP on February 21, 2024, with errors in the TOC graphic. The corrected version was reposted on February 22, 2024.

https://doi.org/10.1021/acs.oprd.3c00448
Org. Process Res. Dev. 2024, 28, 1903−1909